Nanocomposite Mo-Ti-N Coatings for Wear Resistant Applications

D. Glocker, Isoflux Incorporated, Rochester NY; and M. Graham, R. Hoffman, A. Madan, and J.-S. Wang, Northwestern University, Evanston, IL

Key Words: Nanocomposite coatings, Reactive sputtering, Superhard materials, Cylindrical magnetron

ABSTRACT

The objectives of this work were to demonstrate the feasibility of depositing novel nanocomposite coatings using cylindrical magnetron sputtering, to verify their nanocomposite structure, and to relate their mechanical properties to their structure and composition. A large number of nanocomposite coatings with varying Mo and Ti contents were deposited. Key coating properties, including hardness, microstructure, composition, and stability were evaluated using a variety of testing techniques. X-Ray diffraction (XRD) and cross-sectional transmission electron microscopy (XTEM) were used to characterize the microstructure of the coatings. The hardnesses of the coatings were measured using a nanoindenter. The amount of Mo and Ti was estimated using scanning electron microscopy with energy dispersive spectroscopy (EDS). Our results show that we can obtain nano-composite films using both split targets and multiple ring targets with a cylindrical magnetron. By varying the relative area ratio of the rings, we can obtain the desired ratio of the two materials being sputtered. The composition is uniform over the length of the substrate holder when ring targets are used.

INTRODUCTION

One approach to achieving superhard (>50 GPa) coatings is the use of nanolayered nitride structures. For example, hardness values of greater than 50 GPa are achieved in polycrystalline superlattice films of TiN/NbN and TiN/VN when the superlattice period is in the 3 to 5 nm range. This is about a factor of two higher than that of the rule-of-mixtures value [1]. However, this approach has potential problems. The first is the difficulty of maintaining the proper superlattice period over the convoluted surface of some machine tools. The second concerns the stability of the nano-layered structure at high temperatures. For example, annealing TiN/BN multilayer coatings at 800°C resulted in a factor of three decrease in the hardness [1].

An alternative concept for the design of superhard nanocrystalline composite coatings has been suggested using several nc-M_nN/a-Si_3N_4 systems (nc-M_nN is a nanocrystalline transition metal nitride: M= Ti, W, V; a-Si_3N_4 is amorphous silicon nitride) [2–6]. These materials consist of a nanocrystalline hard transition metal nitride embedded in an approximately 1 nm thin matrix of amorphous Si_3N_4. Unlike the heterostructures and nanocrystalline coatings, which show softening when the crystallite size or lattice period decreases below the critical size, the hardness of these composites increased with decreasing crystallite size. One potential disadvantage of this system, however, is the high solubility of silicon in many metals, which limits its use for cutting tools and other applications. These films consist of nanocrystalline particles of about 90% volume fraction in an amorphous matrix. The toughness, cohesion between the coating and the substrate, and structural stability at elevated temperature might also pose problems.

This paper describes the application of the dispersoid hardening mechanism, which is widely adopted in developing ultrahigh strength steels and superalloys, to the development of superhard coatings. The modeled behavior of the Mo-Ti-N system has been experimentally verified using cylindrical magnetron sputtering.

MODELING RESULTS

The dispersoid hardening model was used to determine the predominant factors affecting the hardening in a multi-phase material. Though this mechanism has been widely applied in developing ultrahigh strength steels and superalloys, it has not been used in developing superhard coatings, primarily because of the difficulty in producing a large volume fraction of ultra-fine particles. Physical vapor deposition processes provide the means of creating a highly non-equilibrium mixture of the deposited components. Fine dispersoids are extremely efficient hardeners in crystalline solids.

The possibility of increasing the hardness of TiN and Mo coatings by the introduction of BN and TiN in the respective matrices was investigated. The hardening was modeled as the resistance to the Orowan bowing of dislocations and the shear cutting of particles. Modeling showed that the predominant factors affecting the hardening are the particle size, volume fraction, and the elastic modulus ratio between the particles and the matrix. The results of the modeling for ceramic TiN dispersed in a metallic, crystalline Mo matrix are shown in Figure 1(a). Calculations show that the hardness of Mo may be increased more than 10 times by 30 volume percent of TiN

 505/856-7188

48th Annual Technical Conference Proceedings (2005) ISSN 0737-5921

particles of size about 2.2 nm (Figure 1a). Curve 1 is the effect of the shear cutting of particles by dislocations. Curve 2 is the Orowan bowing resistance to dislocation motion. The theoretically predicted maximum hardness (~ 32 GPa) occurs for the particle size of ~ 2.5 nm and a volume fraction of ~ 0.3. The hardness of pure Mo is about 3 GPa.. The hardness may be even higher if the elastic modulus of the dispersoid is higher (Figure 1b). The modulus ratio is the ratio of the shear modulus of the dispersoid to the shear modulus of the matrix.

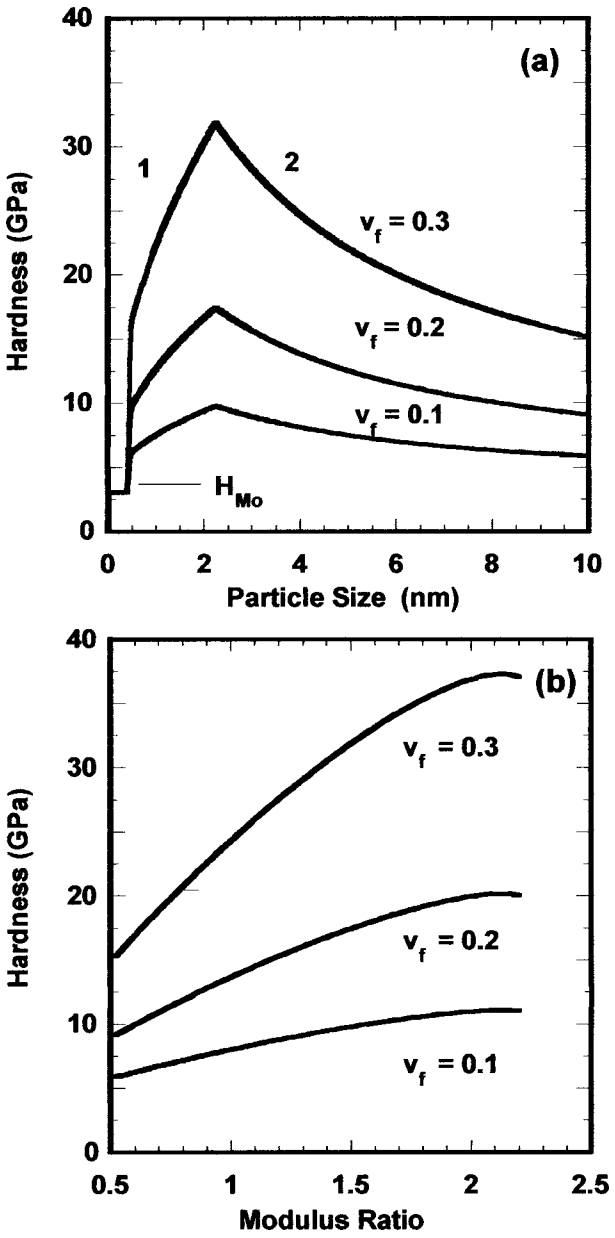

Figure 1. (a) Effect of particle size on the hardness of a nanocomposite film consisting of nanoscale TiN particles dispersed in a Mo matrix. 'v_f' is the volume fraction of the dispersed TiN phase. (b) The theoretically predicted maximum hardness plotted versus the modulus ratio for different volume fractions of the dispersed particles.

EXPERIMENT PROCEDURE AND RESULTS

We chose Mo-Ti-N as a model system to demonstrate the predicted hardening mechanism. The heat of formation of TiN is about a factor of 5 higher than that of MoN, indicating that TiN is much more likely to form during reactive sputtering with nitrogen [7]. This research was focussed on investigating the influence of composition, nitrogen partial pressure, bias voltage and bias current on the microstructure and hardness of the films. A split cathode cylindrical magnetron, shown in Figure 2 in the split target geometry, was used.

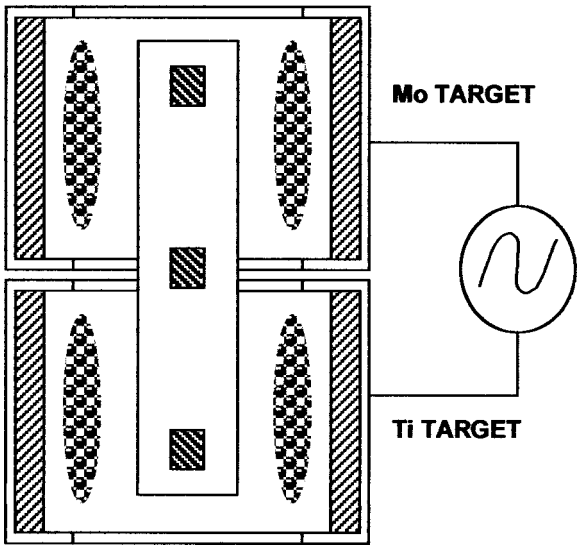

Figure 2. Split cylindrical magnetron cathode configuration used in the preliminary screening experiments. By sputtering the two materials simultaneously as shown, compositionally graded coatings were deposited. Measurements were made for coatings deposited at the three positions in this "split target" geometry.

X-ray diffraction (XRD) was carried out using a Scintag XDS 2000 PAD V diffractometer having an unfiltered CuK radiation source operated at 40 kV and 40 mA. Coating hardness was determined using a CSIRO UMIS2000 nanoindenter fitted with a Berkovitch diamond tip. The system was calibrated using data from a fused silica standard indented with loads in the range of 3 to 50 mN. Analysis of this data followed the method of Oliver and Pharr [8]. Indenter penetration was < 0.1 μm in all cases, <10% of the total film thickness, so that the substrate hardness did not affect the results.

Over 50 samples were made on Si and polished M2 steel substrates under various coating conditions and tested. Preliminary experiments were done to investigate the optimum bias level for deposition of dense films. At the same bias voltage, the bias current was changed by adding or removing wings at the ends of the substrate holder, which acted as a plasma trap through a hollow cathode effect. This led to bias

currents between 260 and 900 mA. A 150 nm TiN buffer was deposited at 0 bias in some cases to improve adhesion.

Monolithic Mo films were deposited using two pure Mo targets. The effect of N_2 and bias on the microstructure and properties were investigated. XRD showed that at 0 bias and in pure Ar, Mo films had a predominant (110) orientation. In Ar/N_2 mixtures, a mixture of Mo(110), Mo_2N(111) and Mo_2N(200) was obtained independent of whether the deposition was at 0 bias or 100V bias. This was a surprising result because the heat of formation of MoN_x is small. Earlier work has shown that metallic Mo is obtained when planar targets are used in an unbalanced magnetron sputtering mode in an $Ar\text{-}N_2$ plasma. The hardness of Mo deposited in the $Ar\text{-}N_2$ plasma was higher (depending on the bias) than that of monolithic Mo deposited in pure Ar. Monolithic TiN deposited by reactive sputtering of Ti in $Ar\text{-}N_2$ atmosphere had a mixed TiN(200) and TiN(111) orientation.

The initial Mo/TiN depositions were done using split targets. Figure 2 shows the split target cylindrical magnetron configuration with Mo on the top and Ti on the bottom. Placement of the substrates at different positions allowed us to study the variation of the composition and hardness with respect to position. In order to determine the reproducibility of our coating process and measurements, replicate coatings were made using split targets operating at 8 mTorr, 5 sccm of N_2 and 50 volts bias. Table 1 shows the results of the hardness and EDS composition measurements at the three positions for these runs. Based on these data, the pooled standard deviation with three degrees of freedom for our hardness measurements was found to be 1.0 GPa and for our compositions was 0.9%.

Table 1. Results of replicated experiments done to verify reproducibility.

Position	Hardness (GPa)		Percent Titanium	
Top	21.1	22.4	13.0	11.7
Middle	24.2	25.7	30.9	31.8
Bottom	26.8	25.3	75.5	74.1

To study the effect of composition, bias voltage and bias current on the film hardness, a designed set of experiments was run. For this set the sputtering pressure was 8 mT and the N_2 flow was 7 sccm. Four bias conditions were used, 50 and 200 volts under high and low current conditions. The results are shown in Table 2. In all of the runs the Ti content in the coatings increased in going from the top to the bottom positions. It can be seen that the hardnesses were affected by bias current and voltage, probably because of changes in the microstructure as well as changes in composition due to re-sputtering.

Table 2. Hardness and percent titanium as functions of bias voltage and current at the top (T), middle (M) and bottom (B) positions with the titanium target in the bottom position.

Bias	Bias	Hardness (GPa)			Percent Titanium		
(V)	(A)	T	M	B	T	M	B
50	0.27	16.2	26.7	22.4	9.6	26.8	74.4
50	0.42	24.7	24.2	18.2	11.8	28.8	75.7
200	0.50	23.5	22.7	22.7	10.6	35.5	76.9
200	0.90	22.0	25.8	18.0	3.9	21.2	70.7

Figure 3 shows the average hardness vs. average composition for the samples at the three positions in this set of runs (points marked A). Point B is the data from samples produced using ring targets, which will be discussed later. The error bars in hardnesses represent the size of the minimum significant factor effect for the *averages* at a 95% confidence level, which is 2.3 GPa based on our replicates. The error bars in Ti content for points A represent the range in compositions measured at each position throughout the experiment. For point B they represent the range in composition from top to bottom, showing good uniformity.

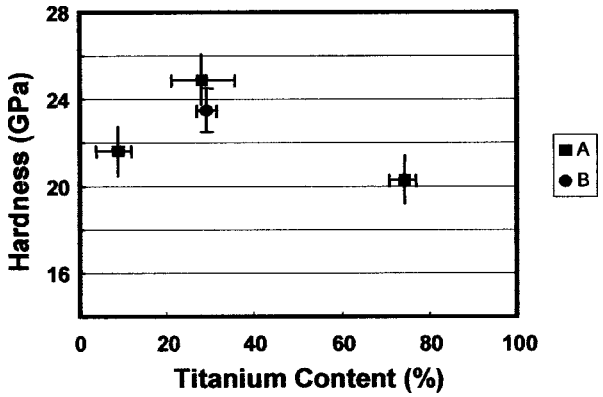

Figure 3. Variation of hardness with the amount of Ti in the coating. Point B is the hardness from samples made using Mo/Ti ring targets with the relative areas chosen to give approximately 30% Ti. The hardness matches closely with the value obtained using split targets having a similar composition.

The data analysis shows that the higher average hardness at the center position is statistically significant at the 95% confidence level. It is also interesting to note that the average hardness at a composition of 30% Ti is 25 GPa, not far from the model predictions as shown in Figure 1a. The model assumed stoichiometric TiN in a pure Mo matrix. Our XRD results indicate some MoN content, so the model is not strictly applicable. However, it is encouraging that the qualitative predictions seem to be correct.

The XRD patterns from the samples described in Table 2 show that different microstructures are obtained, which depend on the amount of Ti and Mo in the film. The composition of the films is affected by the bias, the relative position of the two targets and the sputter yield of the two materials. The XRD analysis is complicated by the fact that there is an overlap of the peak positions in the 2-theta region (36-44°) for Mo, TiN, TiN_x and MoN_x phases. The XRD patterns from the sample in the top position made at high voltage and high current show only a Mo peak and no evidence of Mo_2N peaks. It appears that at these bias conditions, the N_2 has also been resputtered. For the Mo-rich samples at lower bias values, a mixture of Mo, MoN_x and TiN is obtained. The Ti-rich films (bottom) show TiN(200), TiN(111) and TiN_x phases. In the middle position as well as for targets in the ring geometry, the XRD pattern can be best interpreted as a combination of MoN_x, TiN and Mo_9Ti_4 phases.

Dark-field XTEM images were made of a section of a nanocomposite coating deposited in the middle position in the split target geometry. The bias was 100V. The amount of Ti as estimated from the EDS analysis was 30%. Nano-crystalline structures with sizes between 5-20 nm were seen. The rings in selected area diffraction patterns (SAED) correspond to lattice spacings of 0.239, 0.207, 0.151, 0.127, 0.121, 0.105, 0.94 and 0.86 and have an excellent match with TiN (1997 JCPDS 06-0642) and a reasonable match with Mo_2N (1997 JCPDS 25-1366). SAED from a different area of the sample show rings corresponding to lattice spacings of 0.228, 0.201, 0.139, 0.114, 0.98, 0.88, 0.80 and 0.65 and can be best indexed to Mo_9Ti_4(1997 JCPDS 07-0356). The lattice spacings do not match with Mo suggesting that MoN_x has formed. This agrees with the XRD data, which shows that MoN_x forms when Mo is sputtered in a Ar-N_2 atmosphere in our sputtering system.

Following the screening experiments, samples were made using Mo/Ti ring targets with the relative areas chosen to give approximately 30% Ti. The target areas that produced this composition were roughly equal. The sputtering conditions were 8 mTorr, 7 sccm N_2 and 100 volts bias at the high current conditions. The results of the ring target experiments are shown as point B in Figure 3. In this case, the error bars in composition show the range measured for samples made at the top, middle and bottom. The range is small and the agreement is good between the measured hardness for the ring and split targets.

The XRD patterns matched those obtained from the sample placed in the middle position using split targets, which had the same Ti content. This comparison is shown in Figure 4. The peaks are at the same positions confirming that similar microstructures are obtained. This demonstrates our ability to use ring targets to produce compositionally uniform films with the expected values of hardness.

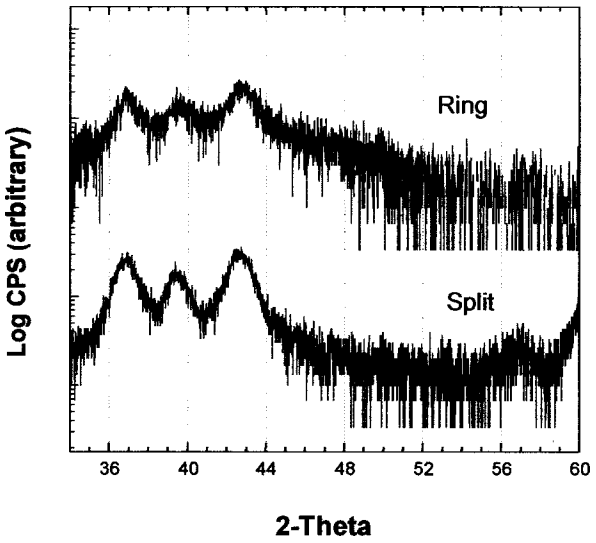

Figure 4. XRD patterns from nanocomposite coatings deposited using the cylindrical magnetron in the a) ring and b) split target geometry.

Preliminary annealing studies were carried out to explore the structural and chemical stability as well as hardness of the nanocomposite coatings at high temperatures. The tip of a cutting tool can reach high temperatures during high-speed operations and it is essential that the coatings retain their hardness. Isothermal annealing was carried out in a furnace in a controlled atmosphere over a temperature range from 500 to 1000°C. Hardness measurements were done after various annealing cycles, and the microstructure changes resulting from the annealing were characterized using x-ray diffraction, allowing a correlation between annealing-induced structure changes and hardness. No measurements could be made on the film annealed at 1000°C since the film delaminated during the anneal, probably because of the difference in the thermal expansion coefficient between the Si substrate and the coating. Within experimental error, the hardness of the films remained constant with annealing up to 750°C. XRD showed that the microstructure was also unchanged. On the other hand, monolithic Mo coatings showed a dramatic decrease in hardness with annealing.

CONCLUSION

We have used cylindrical magnetron sputtering to demonstrate good agreement between a dispersoid hardening model and coatings of Mo-Ti-N. The maximum predicted hardness was 32 GPa at a TiN volume fraction of 0.3 and a particle size of 2.2 nm. The maximum measured hardness was 27 GPa for a coating containing approximately 27% Ti. Transmission electron microscopy showed nanocrystallites of TiN in similar coatings with sizes between 5 and 20 nm. The hardness and structure of the coatings were unaffected by annealing at 750°C.

ACKNOWLEDGMENT

The authors would like to thank the National Science Foundation for their support.

REFERENCES

1. S.A. Barnett, "Deposition and mechanical properties of superlattice thin films," *Physics of Thin Films,* vol. 17, Academic Press, New York, 1993, pp. 2-4.

2. S. Veprek and S. Reiprich, "A concept for the design of novel superhard coatings," *Thin Solid Films*, 268, 64-71, 1995.

3. S. Veprek, P. Nesladek, A. Niederhofer, and F. Glatz, "Search for superhard materials: nanocrystalline composites with hardness exceeding 50 GPa," *NanoStructured Mat.,* 10, 679-689, 1998.

4. S. Veprek, P. Nesladek, A. Niederhofer, F. Glatz, M. Jilek and M Sima, "Recent Progress in the Superhard Nanocrystalline Composites: Toward Their Industrialization and Understanding of the Origin of the Superhardness," *Surf. Coat. Tech.*, 108-109, 138-147, 1998.

5. S. Veprek, P. Nesladek, A. Niederhofer, H. Mannling, **"**Superhard nanocrystalline composites: present status of the research and possible industrial applications," *Surface Engineering: Science and Technology I*, eds. A. Kumar, Y.-W. Chung, J.J. Moore, and J.E. Smugeresky, TMS, 1999, pp. 218-231.

6. J. Musil and P. Zeman, "ZrN/Cu Nanocomposite Film – A Novel Material of the Type Nanocrystalline Metal Nitride/soft Metal Matrix," presented at ICMCTF'99, San Diego, CA, April 1999.

7. O. Kubaschewski and E. L. Evans, *Metal Physics and Physical Metallurgy* (Butterworth-Springer, London, 1951).

8. W.C. Oliver and G.M. Pharr, *J. Mater. Res.* 7, 1564 (1992).